A Novel Sorting Nexin Modulates Endocytic Trafficking and α -Secretase Cleavage of the Amyloid Precursor Protein*

Received for publication, February 25, 2008 Published, JBC Papers in Press, March 19, 2008, DOI 10.1074/jbc.M801531200

Susanne Schöbel $^{\pm 1}$, Stephanie Neumann $^{\pm 1}$, Maren Hertweck $^{\mathbb{S}}$, Bastian Dislich $^{\pm}$, Peer-Hendrik Kuhn $^{\pm}$, Elisabeth Kremmer¹, Brian Seed^{||}, Ralf Baumeister[§]**, Christian Haass[‡], and Stefan F. Lichtenthaler^{‡2}

From the $^{\pm}$ Center for Integrated Protein Science and the Adolf-Butenandt-Institut, Ludwig Maximilians University, Schillerstrasse 44, 80336 Munich, Germany, [§]Center for Biochemistry and Molecular Cell Research (ZBMZ, Faculty of Medicine), Bioinformatics and Molecular Genetics (Faculty of Biology), Institute of Biology 3, and **Center for Systems Biology (ZBSA), University of Freiburg, Schaenzlestrasse 1, 79104 Freiburg, Germany, ¶Helmholtz Center Munich, Institute of Molecular Immunology, Marchioninistrasse 25, 81377 Munich, Germany, and the Department of Molecular Biology, $^{\parallel}$ Massachusetts General Hospital/Harvard Medical School, Boston, Massachusetts 02114

Ectodomain shedding of the amyloid precursor protein (APP) by the two proteases α - and β -secretase is a key regulatory event in the generation of the Alzheimer disease amyloid β peptide $(A\beta)$. β -Secretase catalyzes the first step in $A\beta$ generation, whereas α -secretase cleaves within the A β domain, prevents A β generation, and generates a secreted form of APP with neuroprotective properties. At present, little is known about the cellular mechanisms that control APP α -secretase cleavage and A β generation. To explore the contributory pathways, we carried out an expression cloning screen. We identified a novel member of the sorting nexin (SNX) family of endosomal trafficking proteins, called SNX33, as a new activator of APP α -secretase cleavage. SNX33 is a homolog of SNX9 and was found to be a ubiquitously expressed phosphoprotein. Exogenous expression of SNX33 in cultured cells increased APP α -secretase cleavage 4-fold but surprisingly had little effect on β -secretase cleavage. This effect was similar to the expression of the dominant negative dynamin-1 mutant K44A. SNX33 bound the endocytic GTPase dynamin and reduced the rate of APP endocytosis in a dynamin-dependent manner. This led to an increase of APP at the plasma membrane, where α -secretase cleavage mostly occurs. In summary, our study identifies SNX33 as a new endocytic protein, which modulates APP endocytosis and APP α -secretase cleavage, and demonstrates that the rate of APP endocytosis is a major control factor for APP α -secretase cleavage.

Processing of the type I membrane protein amyloid precursor protein (APP)³ by two different proteases, called α - and β -secretase, is also referred to as shedding and is a central regulatory event in the generation of the amyloid- β peptide (A β), which has a key role in Alzheimer disease (AD) pathogenesis (1). Both α - and β -secretase cleave APP within its ectodomain close to its transmembrane domain (Fig. 1A). The β -secretase is the aspartyl protease BACE1 and cleaves APP at the N terminus of the A β peptide domain, thus catalyzing the first step in A β peptide generation (2). After the initial cleavage of APP by BACE1, the remaining C-terminal APP fragment is cleaved by γ-secretase within its transmembrane domain at the C terminus of the A β domain, leading to the secretion of the A β peptide (3). In contrast to β -secretase, α -secretase cleaves within the A β sequence, and thereby precludes A β peptide generation. The α -secretase is a member of the ADAM family of proteases and may be ADAM10, ADAM17 (TACE), or ADAM9 (4). α and β -secretase are assumed to compete for the ectodomain cleavage of APP (5) but have opposite effects on A β generation. Additionally, α - but not β -secretase cleavage generates a secreted form of APP (APPs α), which has neurotrophic and neuroprotective properties (6-8). Thus, shifting APP shedding away from β - toward α -secretase cleavage could be therapeutically beneficial for AD. In order to do so, it is essential to understand the cellular pathways that control to what extent APP shedding occurs by α - or β -secretase. However, to date little is known about such cellular pathways (9). For example, activation of certain kinases, such as mitogen-activated protein kinase and protein kinase C, increases APP α -cleavage, but it remains unclear how these kinases finally mediate the increase in APP shedding. An additional mechanism controlling APP α and β -secretase cleavage may be the intracellular localization and in particular the endocytic trafficking of APP, which occurs in a clathrin- and dynamin-dependent manner. The α -secretase cleaves mostly at the cell surface, whereas β -secretase cleavage takes place after endocytosis of wild-type APP into endosomes. In fact, APP lacking its cytoplasmic internalization motif accumulates at the plasma membrane and undergoes increased α -secretase but a strongly reduced β -secretase cleavage (10, 11). Likewise, expression of the dynamin K44A mutant,

ferase; SH3, Src homology 3; GFP, green fluorescent protein; PBS, phosphate-buffered saline; AP, alkaline phosphatase; APPs α and APPs β , α -and β -secretase-cleaved APP, respectively.

^{*} This work was supported by a fellowship from the Boehringer Ingelheim Foundation (to S. N.); Deutsche Forschungsgemeinschaft SFB596 Project B12 (to S. F. L.), Project A9 (to C. H.), and Project Z2 (to E. K.); the European Commission for NeuroNE (to C. H.); and the Fonds der Chemischen Industrie (to S. F. L.). The costs of publication of this article were defrayed in part by the payment of page charges. This article must therefore be hereby marked "advertisement" in accordance with 18 U.S.C. Section 1734 solely to indicate this fact.

¹ Both authors contributed equally to this work.

² To whom correspondence should be addressed. Tel.: 49-89-218075453; Fax: 49-89-218075415; E-mail: Stefan.Lichtenthaler@med.uni-muenchen.de.

³ The abbreviations used are: APP, amyloid precursor protein; BAR, Bin/amphiphysin/Rvs; A β , amyloid β peptide; AD, Alzheimer disease; SNX, sorting nexin; PX, Phox homology; HA, hemagglutinin; GST, glutathione S-trans-

which interferes with dynamin-dependent endocytosis in a dominant-negative manner, inhibits APP internalization from the plasma membrane and alters APP shedding. However, conflicting results have been reported as to whether this mainly affects the α - or the β -secretase cleavage or both of them (12, 13). Moreover, expression of Rab5, a key regulator of endocytosis, increases APP internalization from the plasma membrane and enhances APP cleavage by β -secretase, leading to increased A β levels (14). Interestingly, endosomal abnormalities, which are similar to Rab5-overexpressing cells and which are consistent with increased APP endocytosis and cleavage by β -secretase, are among the earliest neuropathological changes observed in AD brain (15), indicating that altered APP endocytosis might contribute to AD pathology. However, the detailed molecular mechanisms controlling APP endocytosis and, thus, the availability of APP for α - and β -secretase are not yet well understood.

Endocytosis in general is a highly coordinated process with a key role in cellular homeostasis (16, 17) and affects distinct properties of cell surface membrane proteins, such as their biological function, signaling, and degradation. A number of different proteins are involved in the orchestration of the endocytic process (17, 18). Among them are the large GTPase dynamin, which is involved in the scission of the endocytic vesicles from the plasma membrane, and the small GTPase Rab5 that is required for the transport of the vesicles and their fusion with the endosomes. However, not all mechanisms controlling endocytosis are understood, and new proteins with a function in endocytic protein trafficking continue to be identified. One such example is sorting nexin 9 (SNX9), a member of the heterogenous family of SNXs (19, 20). SNXs are cytosolic and membrane-associated proteins characterized by the presence of an SNX-type Phox homology (PX) domain, which is a subgroup of the phosphoinositide-binding PX domain superfamily (21). Additionally, SNXs contain a variable number of additional protein-protein and protein-lipid interaction domains (20). At present, few SNXs have been functionally studied, but they are generally assumed to be involved in endosomal trafficking. For example, SNX1 is part of the retromer complex and is involved in the retrieval of the cation-independent mannose 6-phosphate receptor from sorting endosomes (20). SNX9 is involved in endocytosis and binds different endocytic proteins, among them dynamin (22, 23). Whether SNXs contribute to APP endocytosis or processing has not yet been established.

To explore systematically the cellular pathways controlling APP shedding, we employed sib selection expression cloning and identified proteins activating APP shedding by α - or β -secretase. With this approach, we identified a novel member of the SNX family, SNX33, as a new modulator of APP endocytosis and α -secretase cleavage. We find that SNX33 is a novel dynamin-binding protein that inhibits dynamin-dependent endocytosis. Expression of SNX33 reduces the rate of APP endocytosis and increases APP levels at the cell surface, where APP undergoes increased cleavage by α -secretase.

EXPERIMENTAL PROCEDURES

Reagents and Antibodies—The following antibodies were used: anti-HA HA.11 (Covance), anti-HA 12CA5, anti-HA

3F10 (Roche Applied Science), horseradish peroxidase-coupled goat anti-mouse and anti-rabbit (Promega), antibody 6E10 (against A β -(1–17), Senetek Inc.), 6687 (against APP C terminus) (24), 192wt (specific for the C terminus of APPsβ, provided by Dale Schenk), W02 (against amino acids 5–8 of A β , provided by Konrad Beyreuther) (25), anti-dynamin-1/2 (Cell Signaling), anti-dynamin (Hudy1) (Upstate Biotechnology), and anti-Hsp70 (StressGen). Polyclonal SNX33-antiserum 67 was generated against a synthetic peptide (H2N-FRPKPPLERQD-SLASC-CONH₂) within the low complexity domain of SNX33, and control antiserum 92 was generated against an unrelated protein (Eurogentec Seraing, Belgium). Rat monoclonal antibodies 2A1 (IgG1, binding to the SH3 domain of SNX33) and 6C6 (IgG1, binding to the SH3 domain of SNX9) were generated by immunization with GST-SNX33 and GST-SNX9. Control rat antibody 7H8 (IgG1) was against mouse C1q.

Plasmid Construction—cDNAs encoded human proteins. BACE1 (two clones differing in the length of the 3'-untranslated region (26)), SNX33, and dynamin-1 Δ NT were obtained in the peak8 vector from a human brain cDNA library (Edgebio). SNX33 sequence was deposited to GenBankTM (accession number EF653821 (nucleotide), ABV26009 (protein)). Its 5'-untranslated region is 166 bases longer than NM_153271 and has a 3'-untranslated region of 1413 bp. Plasmids pCEP4/ APP695 (27) and peak12/ADAM10 (28) were described. cDNAs of GFP, SNX9 (from ATCC), SNX33 (without untranslated regions or with C-terminal fusions to GFP and HA tag or lacking the SH3 domain), dynamin-1 (C-terminal fusions to HA tag or GFP), protein kinase $C\alpha$ (C-terminal HA tag), and the SH3 domain of SNX33 were generated by PCR and cloned into vector peak12. GST fusions of SNX33 or SNX33-SH3 domain were in pGEX5.1 vector. pSuperHygro was designed to contain a hygromycin resistance cassette in the original multiple cloning site. pSuperHygroSNX33RNAi1 and -2 have the short hairpin RNA sequence 5'-gcacatgatgcagaactac-3' and 5'-ggccgagccctctatgact-3'. Peak8/MEKK2 (encoding constitutively active MEKK2) was described (29). pCB1/dynamin-1 and Dyn-1K44A were obtained from Marc Caron. The identities of all constructs obtained by PCR were confirmed by DNA sequencing. Peak12/ MMP-GFP was described (28), and peak12/MMP-SNX33-IRES-GFP was generated by cloning the SNX33 cDNA into peak12/MMP-IL-1R2-IRES-GFP (30).

Cell Culture, Expression Cloning, Western Blot, APP, and Transferrin Uptake Assays—Human embryonic kidney 293-EBNA (HEK293) and COS cells were cultured as described (30). Clonal HEK293 cells expressing AP-APP and Bcl-X_I/ CrmA (clone Sabc70) were generated as described (28, 31). HEK293 cells stably expressing peak12/AP-L-selectin and peak12/AP-TNFR2 were described (28, 29). Polyclonal HEK293 cells stably expressing pSuper plasmids were selected with 100 μg/ml hygromycin. Polyclonal COS cells stably expressing APP695 were selected in 3.0 μ g/ μ l hygromycin. Transfections were done using Lipofectamine 2000 (Invitrogen). One day after the transfection, medium was changed. After additional overnight incubation, cell lysates (in 50 mm Tris, pH 7.5, 150 mm NaCl, 2 mm EDTA, 1% Nonidet P-40) and media were collected and analyzed. Cells stably expressing pSuper vectors (SNX33 knockdown) were prepared in the same



way. For the indicated experiments, phosphatase inhibitors (50 mм NaF, 1 mм NaVO₄, phosphatase inhibitor (1:100; Sigma)) were added to cell lysates. The expression cloning screen was carried out as described (31). To detect secreted and cellular APP or other cellular proteins, protein concentration in the cell lysate was measured, and corresponding aliquots of lysate or medium were separated by SDS-PAGE. Measurement of alkaline phosphatase (AP) activity, APP and transferrin uptake assays, and image acquisition were performed as described (31,

Preparation of Brain Homogenate, Cytosol, and Membrane Fraction from HEK293 Cells—Mouse brain was homogenated in brain lysis buffer (5 mm Tris, pH 7.4, 250 mm sucrose, 5 mm EGTA, protease inhibitors), centrifuged at 7,000 rpm. Supernatant was centrifuged at $100,000 \times g$ for 60 min (4 °C). Pellet was resuspended in brain lysis buffer containing 1% Triton X-100 and centrifuged at 100,000 \times g (30 min, 4 °C). Cytosol and membrane fractions of HEK293 cells were prepared as described (22) under slightly modified conditions. Briefly, HEK293 cells were seeded in 10-cm dishes. After 72 h, cells were scraped using PBS plus 25 mm EDTA, washed once with PBS, centrifuged at 350 \times g, and washed twice with KSHM buffer (100 mm KCH₃COO, 20 mm HEPES/KOH, pH 7.4, 1 mm Mg(CH₃COO)₂, 85 mm sucrose, 50 mm NaF, 1 mm NaVO₄, phosphatase inhibitor (1:100; Sigma)). Cells were centrifuged at $850 \times g$, resuspended in KSHM buffer, quick frozen in liquid nitrogen, and thawed in a 37 °C water bath twice (the volume of KSHM buffer used was equivalent to the volume of centrifuged cells). Cells were centrifuged; supernatant of opened cells was collected and subjected to ultracentrifugation for 30 min at 4 °C and $100,000 \times g$. Aliquots of the resulting supernatant (cytosol) were frozen in liquid nitrogen and stored at -80 °C. Pellet was resolved in lysis buffer, incubated on ice for 20 min, and centrifuged for 5 min at 4 °C and 13,000 rpm. This supernatant (membrane fraction) was stored at −20 °C. Before immunoprecipitation, cytosol and membrane fraction were ultracentrifuged at 4 °C for 30 min and 100,000 \times g. Additionally, 1% Nonidet P-40 was added to the cytosolic fraction to reduce nonspecific binding in the immunoprecipitation.

Immunoprecipitations and Dephosphorylation—For SNX33/ dynamin co-immunoprecipitation, phosphatase inhibitors (described above) were added to the cell lysates. Lysates were incubated with 5 µg of antibody (anti-HA (12CA5) or antidynamin-1 (Hudy1)) for 4 h (4 °C) using protein-G Dynabeads (Dynal). After washing with STEN-NaCl (STEN buffer plus 0.35 м NaCl) and twice with STEN (0.05 м Tris/HCl, pH 7.6, 0.15 M NaCl, 2 mm EDTA, and 0.2% Nonidet P-40), bound proteins were resolved by SDS-PAGE. For anti-HA immunoprecipitations (HA.11, for the dephosphorylation experiment) lysates were incubated with antibody (300:1) and treated or not with shrimp alkaline phosphatase (Roche Applied Science) overnight at 37 °C in the presence of protease inhibitors. For SNX33 immunoprecipitation, antibody 67 (polyclonal) was used at a 1:100 dilution or antibody 2A1 (monoclonal) was used at a 1:10 dilution with protein-A- and protein-G-Sepharose, respectively.

Cell Surface Biotinylation—48 h after transfection, HEK293 cells (in poly-L-lysine-coated 24-well dishes) were washed on

ice three times with ice-cold PBS and incubated for 30 min on ice with PBS containing 0.5 mg/ml EZ-linkTM-Sulfo-NHS-SS-Biotin (Pierce). Cells were washed three times with ice-cold 20 mM glycine plus PBS. The last wash was left for 15 min on cells (on ice). After three additional washes with ice-cold PBS, cell lysates were prepared. To detect biotinylated APP, protein concentration in the cell lysate was measured, and corresponding aliquots of lysate were used for immunoprecipitation overnight at 4°C using Streptavidin-Sepharose High Performance (Amersham Biosciences).

Northern Blot Analysis—Multiple-tissue Northern blot analysis was performed according to the supplier's protocol (Clontech, BD Biosciences). Briefly, a $[\alpha^{-32}P]dCTP$ (Amersham Biosciences)-labeled SNX33 or actin probe (Random Primer DNA Labeling System; Invitrogen) was added to a human multipletissue Northern blot (BD Biosciences). Hybridization was performed overnight at 65 °C. Excess probe was removed by washing with $2 \times$ SSC, 0.1% SDS at room temperature, followed by washing with 0.1× SSC, 0.1% SDS at 65 °C. The blot was exposed to Super RX film (Fuji).

Purification of GST Fusion Proteins and GST Pull-down-GST proteins were expressed in Escherichia coli BL21 cells and purified according to the manufacturer's protocol (Amersham Biosciences). GST-SNX33 was eluted using 8 M urea. For in vitro binding studies, HEK293 lysates were incubated with 30 μ l of GST or GST-SH3 fusion protein coupled to GSH-Sepharose beads. Equal amounts of GST and GST-SH3 fusion protein were used (estimated by Coomassie Blue staining). Samples were incubated at 4 °C for 2 h and washed five times with 1 ml of STEN buffer. Co-precipitated dynamin was detected using dynamin-1/2 antibody.

Retroviral Transduction—For the transduction of HeLa cells and H4 neuroglioma cells, retroviral supernatants (replicationdeficient Moloney murine leukemia virus) were generated as described (30), using peak12/MMP-GFP or peak12/MMP-SNX33-IRES-GFP.

Trichloroacetic Acid Precipitation—One confluent 10-cm dish was lysed in 800 μ l of solubilization buffer. 88 μ l of 50% trichloroacetic acid solution were added. After a 10-min incubation on ice, precipitate was pelleted in a microcentrifuge and washed twice with ice-cold acetone. Pellet was dried in heat block (50 °C), resuspended in 2.3× sample buffer containing 6 м urea, and heated for 10 min at 95 °C. Trichloroacetic acid precipitate was resolved on 10% acrylamide gels containing 2.8 M urea and subject to immunoblot analysis.

Caenorhabditis elegans Strains—The following strains were used: N2 Bristol (wild type), CX51 dyn-1(ky51), BR3380 Ex[lst-4::gfp] line 1, BR3381 Ex[lst-4::gfp] line 2, ZH301 Ex[dyn-1a/b::gfp], BR4825 Ex[dyn-1a/b::gfp; lst-4::gfp].

lst-4::gfp Expression—A lst-4::gfp translational fusion was constructed by cloning a 2.4-kb upstream regulatory sequence and complete cDNA of lst-4 (Y37A1B.2c) into pPD95.75 (A. Fire; Carnegie Institute of Washington, Baltimore, MD). 20 $ng/\mu l$ was injected into N2 together with rol-6 (pRF4; 80 $ng/\mu l$) as coinjection marker (33). The injection yielded two independent transgenic lines (BR3380 and BR3381) that were used for further functional analysis. To generate BR4825 for rescue



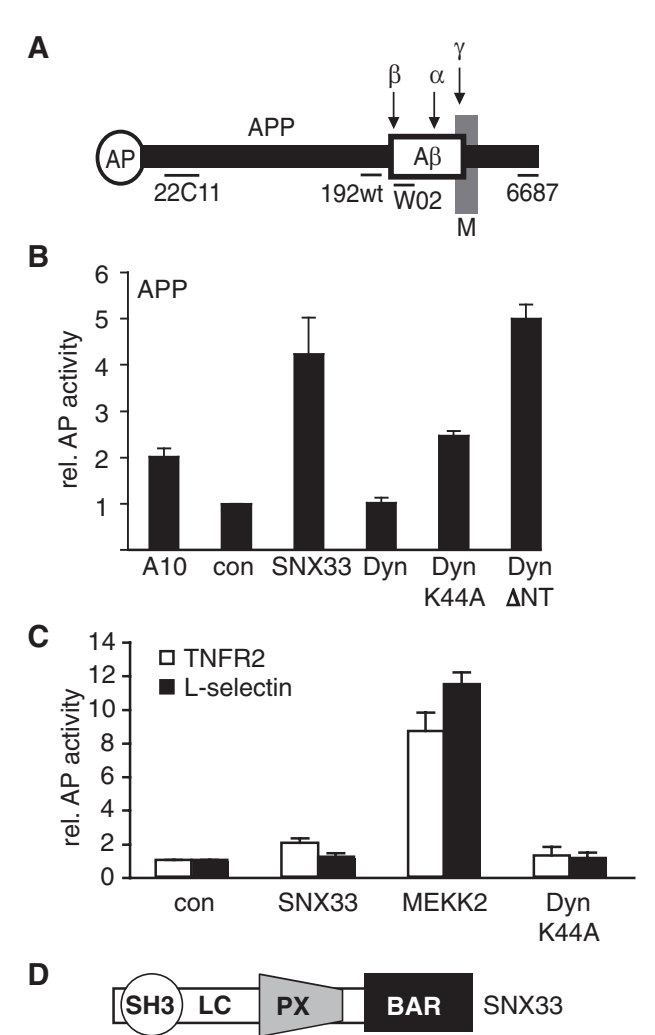


FIGURE 1. SNX33 expression stimulates APP shedding. A, schematic drawing of APP. The horizontal bars show the localization of the epitopes recognized by the indicated antibodies. The arrows point to the proteolytic α -, β -, and γ -secretase cleavage sites within the APP ectodomain or transmembrane domain. Sequential cleavage of APP by β - and γ -secretase generates the A β peptide (white box). AP, alkaline phosphatase; M, membrane. B, AP reporter assay for the ectodomain shedding of APP. Human embryonic kidney 293 cells stably expressing AP-tagged APP were transiently transfected with the indicated constructs. AP activity in the conditioned medium was measured relative to control-transfected cells. Shown are mean and S.D. of three independent experiments. A10, ADAM10; Con, control; Dyn, dynamin-1. C, 293 cells stably expressing the AP-L-Selectin or AP-TNFR2 fusion protein were transiently transfected with the indicated constructs. Alkaline phosphatase activity was measured in the conditioned medium of the cells. Shown are the mean and S.D. of three independent experiments, each one carried out in duplicate. D, domain structure of SNX33. LC, low complexity.

experiments, Ex[lst-4::gfp] (BR3380) was crossed into Ex[dyn-1a/b::gfp] (ZH301).

RESULTS

Identification of SNX33 in an Expression Cloning Screen for Activators of APP Shedding—To identify new modulators of APP shedding by α - or β -secretase, an expression cloning screen was performed. To this aim, cDNAs of an unamplified human adult brain cDNA library were transfected into a reporter cell line, which allows rapid detection of APP shedding in a high throughput format. The reporter cell line consists of human embryonic kidney 293 (HEK293) cells, which stably express a fusion protein of AP and full-length APP (AP-APP)

(Fig. 1A) (31). Upon cleavage of APP by α - or β -secretase, the secreted fusion protein can be detected in the conditioned medium by measuring the AP activity (28, 31). To protect the cells against possible cell death induced by proapoptotic genes represented in the cDNA pools, the HEK293 cells were additionally transfected with a plasmid encoding the cDNAs of two antiapoptotic proteins, Bcl-X_L and CrmA. Three cDNAs were obtained, which increased AP-APP secretion at least 4-fold compared with control-transfected cells. They had a stronger effect on APP shedding than the well characterized α -secretase ADAM10, which was used as a positive control and increased shedding 2-fold (Fig. 1B). First, the known APP β -secretase BACE1 (34) was identified, which validates the screening approach, since it shows that cDNAs can be obtained that are physiologically relevant for APP shedding. Second, a partial cDNA of the endocytic GTPase dynamin-1 was identified, encoding a truncated dynamin-1 lacking the N-terminal 209 amino acids, including the GTPase domain (Dyn Δ NT). This protein is expected to act as a dominant negative dynamin mutant (35). DynΔNT increased AP-APP shedding 5-fold and had an even stronger effect than the well characterized dynamin-1 K44A mutant (Fig. 1B), which was previously shown to inhibit APP endocytosis and increase APP shedding (12, 13). As a control, expression of wild-type dynamin, which does not inhibit endocytosis, did not affect APP shedding (Fig. 1B). A third cDNA encodes a protein, which is identical to an as yet uncharacterized protein annotated as SNX33 or SH3PX3 (36). SNX33 increased APP shedding 4-fold (Fig. 1*B*). It did not affect the shedding of the corresponding AP fusion protein of the cell adhesion protein L-selectin (Fig. 1C) but increased the shedding of TNFR2 (tumor necrosis factor- α receptor 2) by 2-fold. L-selectin and TNFR2 undergo an α -secretase-like shedding similar to APP (28, 37, 38). As a control, to show that the shedding of L-selectin and TNFR2 can be enhanced in this assay, we used the kinase MEKK2, which strongly activated the shedding of both proteins (Fig. 1C). The novel protein SNX33 comprises 574 amino acids and has an N-terminal SH3 domain followed by a low complexity region (LC), a central phosphoinositidebinding PX domain, and a C-terminal BAR (Bin/amphiphysin/ Rvs) domain (Fig. 1D). SNX33 has two distant homologs, SNX9 (35.9% identity) and SNX18 (42.6% identity), which share the same domain structure (sequence alignment shown in Fig. 2). Although SNX18 has not yet been studied, SNX9 is involved in multiple modes of endocytosis and binds different endocytic proteins, including dynamin (22, 23, 39-42).

Expression Pattern and Phosphorylation of SNX33—Multiple-tissue Northern blot analysis revealed ubiquitous expression of SNX33, with a strong expression in heart and pancreas (data not shown). Endogenous SNX33 protein was detected in mouse brain homogenate (Fig. 3A) and HEK293 cells (Fig. 3B) as well as neuroblastoma SH-SY5Y cells, HeLa cells, neuroglioma H4 cells, and hepatoma HepG2 cells (data not shown) and has an apparent molecular mass of 70 –75 kDa (Fig. 3B), which is slightly above its calculated molecular mass of 65 kDa. When cell lysis was carried out in the presence of phosphatase inhibitors, SNX33 was detected as a doublet band (Fig. 3B). These bands could be converted to a single band by treatment with alkaline phosphatase (Fig. 3C), revealing that SNX33 is a phos-

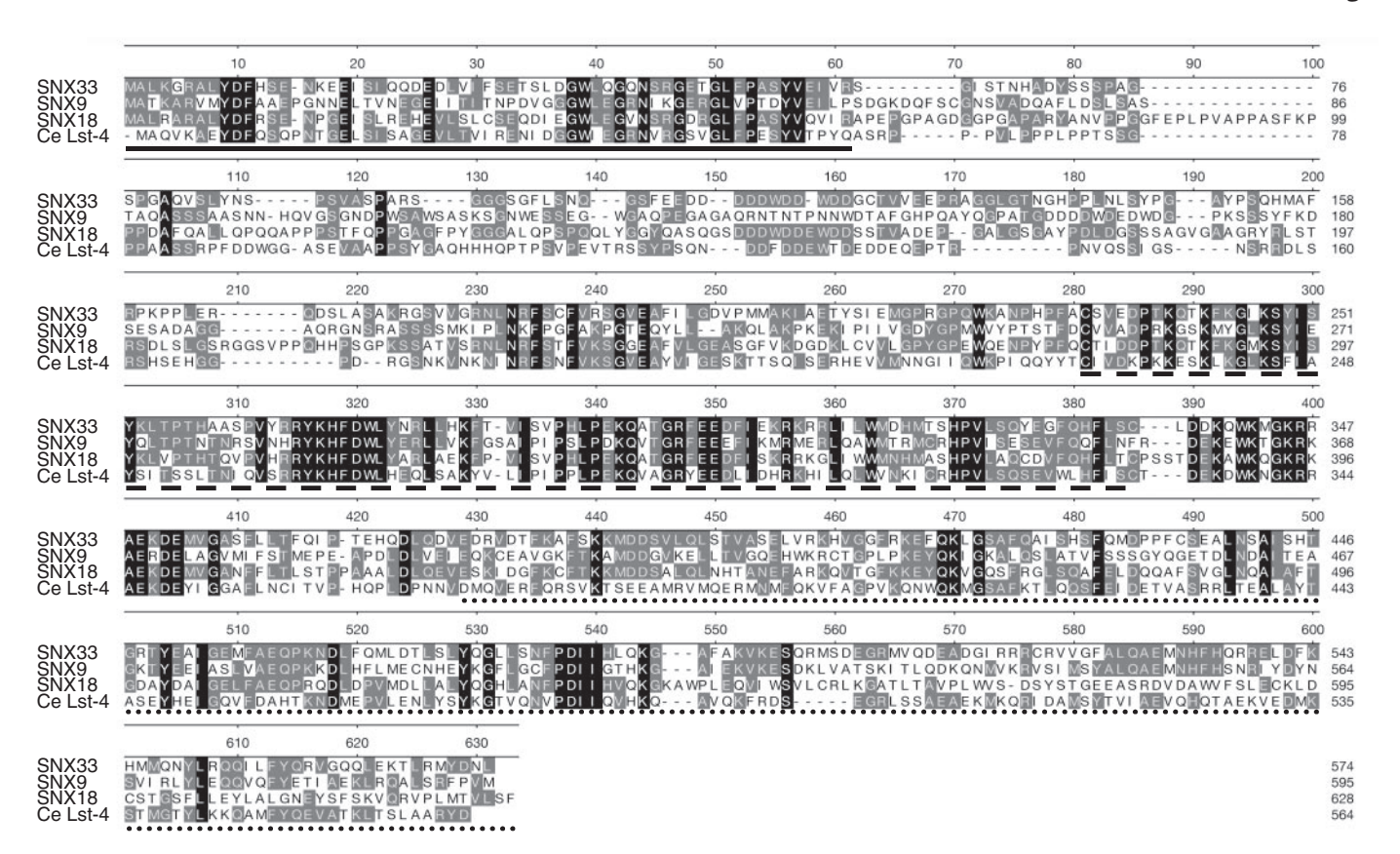


FIGURE 2. Sequence alignment of SNX33 and its homologs. Alignment of the protein sequences of human SNX33 (574 amino acids) and its human homologs SNX9 (595 amino acids) and SNX18 (628 amino acids) and of the single C. elegans ortholog LST-4 (564 amino acids; splice form Y37A1B.2d). SH3 (continuous line), PX (dashed line), and BAR (dotted line) domains are underlined. SNX33 shares 35.9% identity (49.6% similarity) with SNX9 and 42.6% identity (54.6% similarity) with SNX18. C. elegans LST-4 is slightly more homologous to human SNX33 (52.5% similarity) than to SNX9 (48.2% similarity) and SNX18 (48.6% similarity), as determined with the EMBL EMBOSS-Align software tool.

phoprotein. Fractionation of HEK293 or SH-SY5Y cells into membrane fraction and cytosol revealed that SNX33 is found in both fractions (Fig. 3, B and D; shown for HEK293 cells). The partial membrane association of SNX33 is in agreement with the presence of a PX and a BAR domain that are also found in other membrane-associated proteins (43).

SNX33 Activates α -Secretase Cleavage of APP—Next we determined whether SNX33 stimulated APP shedding by increasing α - or β -secretase cleavage. SNX33 was transiently transfected into HEK293 cells and retrovirally transduced into HeLa cells and H4 neuroglioma cells expressing endogenous APP. Secreted APP was detected in the conditioned medium using cleavage site-specific antibodies. Antibody W02 detects α -secretase-cleaved APP (APPs α) and revealed a strong increase in APP α -cleavage upon SNX33 transfection into all three cell lines (Fig. 4A). For the HEK293 cells, the increase was 3-fold (Fig. 4B), which agrees well with the 4-fold increase in APP shedding observed in the AP-APP reporter cell line (Fig. 1B). Antibody 192wt specifically detects β -secretase cleaved APPs (APPs β). APPs β was slightly increased in HEK293 cells (Fig. 4A; quantification in Fig. 4B) but was not significantly increased in HeLa or H4 cells (not shown). The amount of A β derived from the endogenous APP was below the detection limit. Expression of SNX33 did not alter the total amount of APP in the cell lysate. Expression of Dyn K44A in HEK293 cells had the same effect as SNX33. It increased APPs α and did not

have a major effect on APPs β (Fig. 4C). A C-terminal HA epitope tag or a fusion to GFP did not alter the effect of SNX33 on APP α -cleavage (Fig. 4D). The SNX33 homolog SNX9 had a similar effect on APP shedding as SNX33 (Fig. 4D), suggesting that both proteins are functional homologs, at least with regard to APP shedding. Taken together, SNX33 strongly increases APP α -cleavage but only has a minor effect on APP β -cleavage. The increase in APP α -shedding required the presence of the SH3 domain of SNX33, because a SNX33 deletion mutant lacking the SH3 domain had largely lost the ability to stimulate APP α -secretase cleavage (data not shown). To test whether the SH3 domain alone would be sufficient to increase the α -secretase cleavage, we expressed the SH3 domain or full-length SNX33, both fused to GFP. As expected, full-length SNX33-GFP increased α-secretase cleavage compared with GFP or mocktransfected cells (Fig. 4E). However, SH3-GFP had largely lost the ability to stimulate α -secretase cleavage. Taken together, these experiments reveal that the SH3 domain of SNX33 is necessary but not sufficient for the effect on APP shedding. Because the SNX33 homolog SNX9 dimerizes through its C-terminal BAR domain (44), it is possible that SNX33 requires its BAR domain and must be able to dimerize for full activation of APP α -secretase cleavage. Likewise, SNX9 requires both its SH3 domain and more C-terminal domains to efficiently stimulate the GTPase activity of dynamin (23).

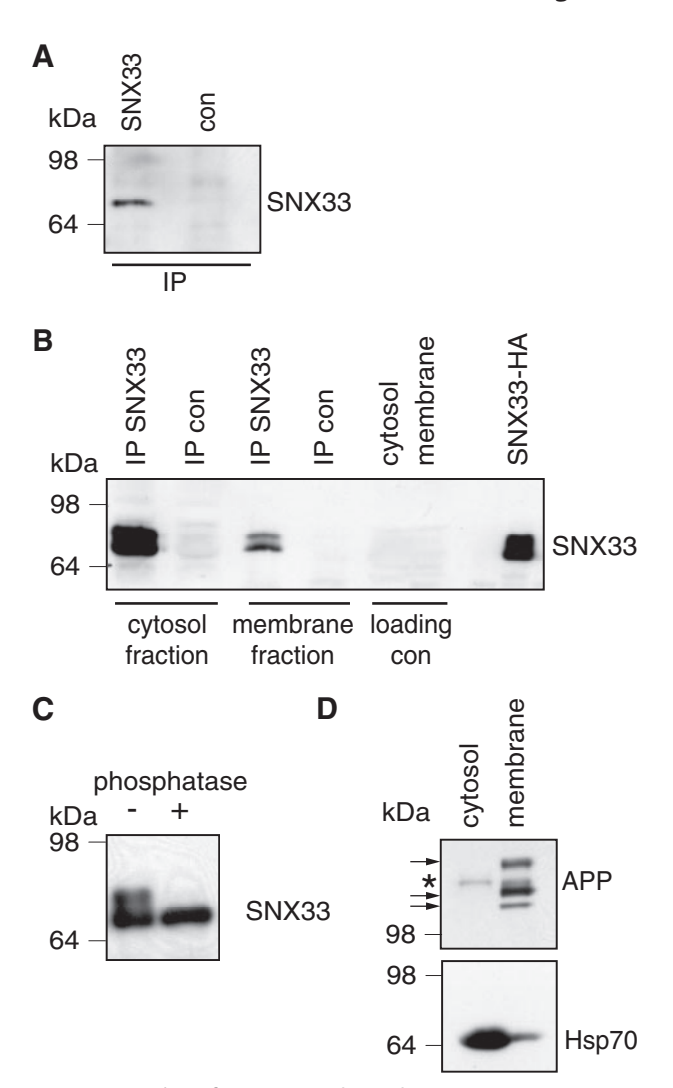


FIGURE 3. Expression of SNX33. A and B, endogenous SNX33 was immunoprecipitated from mouse brain (A) or from cytosol and membrane fraction of HEK293 cells (B). SNX33 was only detected when immunoprecipitation (IP) was carried out with SNX33-specific (67 in A, 2A1 in B) but not with a control antiserum (con) against an unrelated protein. For immunoblot detection, SNX33 antibody 2A1 was used. Without immunoprecipitation, SNX33 is not detected in directly loaded cytosol and membrane fraction (loading control) (B). As a control, cell lysate of SNX33-HA-transfected HEK293 cells (SNX33-HA) was loaded in the right lane of B. C, dephosphorylation of transfected SNX33 immunoprecipitated from HEK293 cells converts the upper protein band to the lower one, indicating that SNX33 is partly phosphorylated. D, to test for specificity of cell fractionation, cytosolic and membrane fractions in B were reprobed for APP (membrane protein found only in membrane fraction) with antibody 22C11 and Hsp70 (soluble protein, found predominantly in the cytosol fraction). *, nonspecific background band. The arrows indicate mature and immature forms of the two endogenous APP isoforms APP695 and APP751, which differ in their length.

Next, we analyzed how a knockdown of SNX33 affects APP shedding. HEK293 cells with a stable knockdown of SNX33 were generated, using two independent short hairpin RNA sequences. Compared with control cells, no difference in APP shedding was observed in the SNX33 knockdown cells (Fig. 4F). This is probably due to the fact that in the absence of SNX33, the homologous SNX9 (and probably also SNX18) is still present. SNX9 was found to be expressed at 10-20 times higher protein levels than SNX33, as determined in HEK293 and neuroglioma H4 cells, respectively (Fig. 4, G and H).

SNX33 Expression Reduces Endocytosis of APP and the Uptake of Transferrin—The mutant DynK44A, which inhibits APP endocytosis (12, 13, 32, 45), had a similar stimulatory effect on APP shedding (Fig. 1B) and on APP α - and β -secretase cleavage (Fig. 4C) as SNX33. Based on this finding, we speculated that SNX33 expression may also inhibit APP endocytosis, leading to increased APP levels at the cell surface, where the α -secretase cleavage is assumed to take place (46). To test this hypothesis, we used a validated immunofluorescence-based anti-APP antibody uptake assay (32). COS cells were transiently co-transfected with APP and either GFP, as a control, or GFPtagged SNX33 (SNX33-GFP; Fig. 5A). In this assay, APP showed a typical cell surface staining at 0 min (patchy cell surface staining and partly bright rim of the cell; Fig. 5A). At later time points, numerous cells showed APP-containing vesicles, which we have previously shown to be EEA1-positive, identifying them as endosomes (32). Transfected cells were identified by their green fluorescence (GFP or SNX33-GFP) and scored as either showing endocytosis (endocytic APP-positive vesicles; Fig. 5A) or not showing endocytosis (patchy cell surface APP staining and no endocytic vesicles; Fig. 5A). Because not all cells start endocytosis at the same time, around 100 cells at every time point were analyzed and scored. Representative pictures for 0, 7, and 20 min are shown in Fig. 5A (quantitative analysis in Fig. 5B). At time point 0 min, none of the SNX33- or controltransfected cells showed endocytosis (Fig. 5B), as seen by the typical cell surface staining of APP (Fig. 5A). At 7 min, nearly 60% of the control cells had endocytosed APP, whereas this was the case for only about 30% of the SNX33-transfected cells, indicating that SNX33 expression lowered the rate of APP endocytosis. At 20 min and at 35 min, APP endocytosis increased in the control and the SNX33-transfected cells. At 35 min, essentially all control cells displayed APP endocytosis, whereas only 50% of the SNX33-transfected cells showed endocytosis at this time point (Fig. 5B). This reveals that SNX33 expression does not completely inhibit APP endocytosis but strongly slows down the rate of APP endocytosis. In this transient transfection experiment, some cells expressed only APP and not the GFP-tagged SNX33 (Fig. 5A, indicated with arrowheads at 7 and 20 min). Similar to the control-transfected cells, these cells showed endosomal APP staining, whereas at the same time point the SNX33-expressing cells still showed cell surface APP staining (at 7 min, arrows) or only started to show APP endocytosis (at 20 min, arrows).

Consistent with the reduction of APP endocytosis, SNX33 increased APP cell surface levels 2-fold compared with controltransfected cells, as determined by cell surface biotinylation of HEK293 cells (Fig. 5, C and D). The same effect was observed for expression of the SNX33 homolog SNX9 (not shown). Together, these results indicate that SNX33 increases APP α -cleavage by reducing APP endocytosis and increasing the availability of APP at the cell surface. Exogenous expression of SNX33 also inhibited the uptake of fluorescently labeled transferrin (Fig. 6A; quantification in Fig. 6B), which is a measure for the rate of transferrin receptor endocytosis. Both strongly and weakly SNX-GFP-expressing cells showed cell surface staining of transferrin, whereas neighboring cells in the same picture (not expressing SNX33-GFP) or control cells (GFP; not shown)



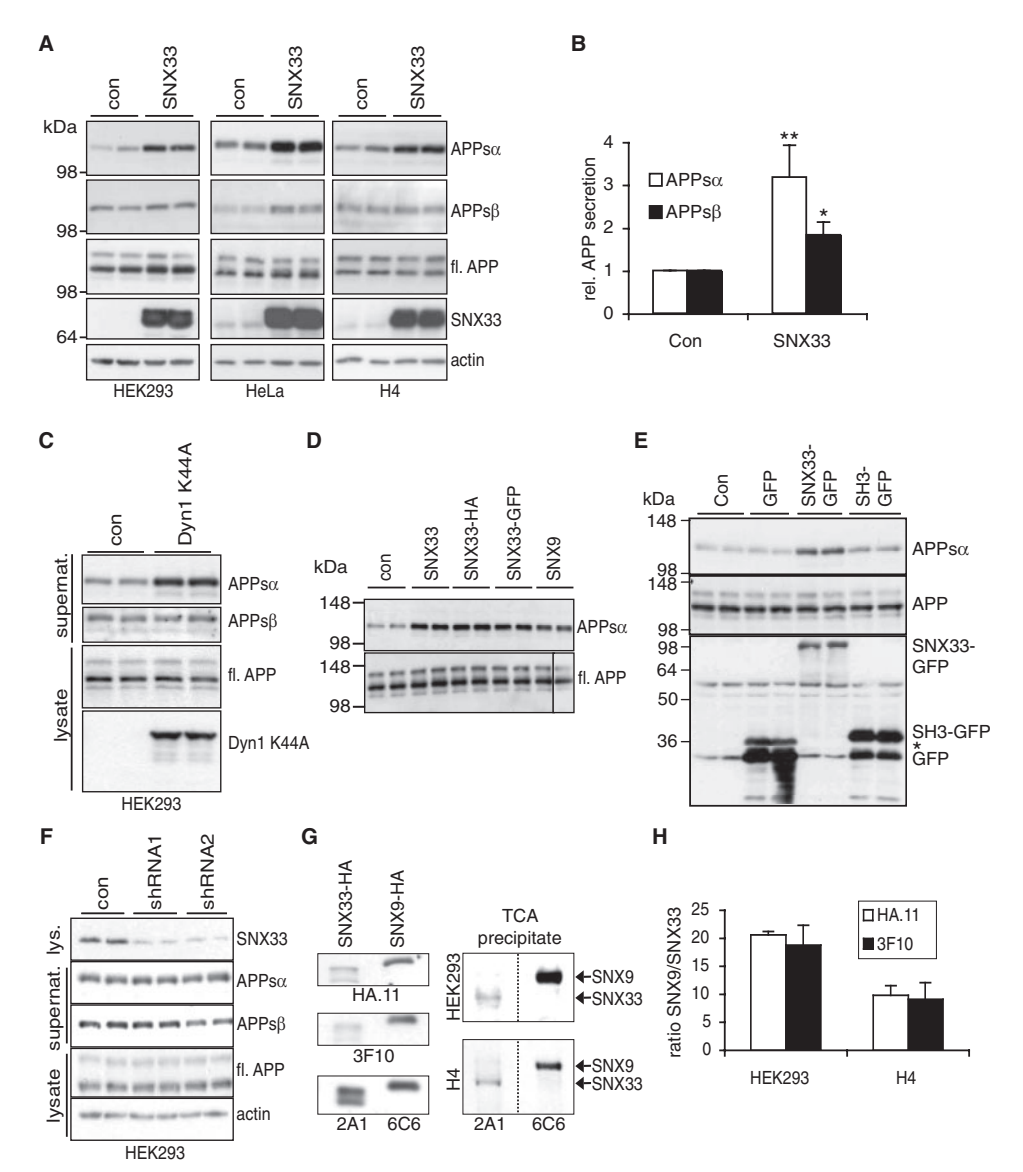


FIGURE 4. **SNX33 increases** α -secretase cleavage of APP. A, HEK293, HeLa, and H4 cells were transiently transfected or transduced with SNX33-HA or with a control vector in duplicates. Aliquots of the conditioned medium and of the cell lysate were analyzed by immunoblot analysis. Soluble APP in the conditioned medium was detected using antibody W02 (detecting APPs α) and antibody 192wt (detecting the β -cleaved APP APPs β) (see Fig. 1A for epitopes). The total amount of APP in the cell lysate was detected using antibody 6687, and expression of the transfected construct was shown using HA antibody. Shown are representative blots of at least three independent experiments. B, quantification of the results from HEK293 cells in A. Shown are mean and S.D. from four independent experiments, each one carried out in duplicate. Values are relative to the secretion of APPs α and APPs β in control cells. C, experiment as in A. Dynamin-1 K44A-HA (Dyn1 K44A) was transfected into HEK293 cells. D, C-terminal HA or GFP tags do not alter the stimulatory effect of SNX33 on APP shedding. SNX9 has a similar effect on APP shedding as SNX33. Experiments were carried out as in A. APPs α and fl.APP were detected with W02 antibody. E, the indicated constructs were transfected into HEK293 cells and analyzed as in A. The band labeled with an asterisk (lower panel, GFP lanes) is likely to represent a dimer of a GFP degradation product and is only seen upon long exposure. F, HEK293 cells stably transfected with pSuper vector or pSuper vector carrying short hairpin RNAs against SNX33 were analyzed as in A for APP shedding. G, determination of the protein expression level of SNX9 relative to SNX33 in HEK293 and neuroglioma H4 cells. Antibodies used for blotting are shown below the panels. Left panels, comparison of the sensitivities of the antibodies. C-terminally HA-tagged SNX33 and SNX9 were transiently expressed in HEK293 cells. Identical aliquots of cell lysate were analyzed with two different anti-HA tag antibodies (HA.11 and 3F10) or with antibodies specific for SNX33 (2A1) and SNX9 (6C6). Band intensities of 2A1 and 6C6 were normalized for band intensities of the HA-antibodies; antibody 2A1 gives a 2-fold higher band intensity than 6C6 (2.0-fold when normalized to HA.11 and 1.8-fold when normalized to 3F10). Right, trichloroacetic acid (TCA) precipitation and detection of endogenous SNX33 and SNX9 from HEK293 and H4 cells. Samples were resolved on a 10% urea gel and immunoblotted with antibody 2A1 (SNX33) or 6C6 (SNX9). Dotted vertical lines indicate that samples were run on the same gel but detected with the indicated different primary antibodies. H, quantification of results from G. Band intensities of 2A1 and 6C6 signals of trichloroacetic acid precipitations were quantified and corrected for the fact that 2A1 gives a 2-fold stronger signal than 6C6 (see F; normalized to the two different HA-antibodies). Ratios of corrected 6C6/2A1 were determined. Shown is the amount of the two different HA-antibodies and the state of theof endogenous SNX9 compared with endogenous SNX33 protein levels (10-20 times more SNX9 than SNX33). Shown are mean and S.D. of three independent experiments.

clearly accumulated transferrin in intracellular vesicles (Fig. 6A). Together, these experiments show that SNX33 can influence the endosomal trafficking of cell surface proteins. Additionally, the experiments reveal that SNX33 expression results in a more general inhibition of endocytosis and mimics a dynamin loss-of-function phenotype similar to the DynK44A mutant.

SNX33 Binds to Dynamin-SNX33 may bind and inhibit endogenous proteins involved in endocytosis, thereby causing the reduction of APP endocytosis and the dynamin loss-of-function phenotype. Such a binding partner of SNX33 could be dynamin itself, which is supported by three findings. First, SNX33 co-immunoprecipitated with dynamin-1 but not with the unrelated protein, protein kinase $C\alpha$ (as a control for specificity), from transfected HEK293 cells (Fig. 7A). This interaction required the SNX33 SH3 domain, because a SNX33 SH3 deletion mutant showed interaction no with dynamin (Fig. 7A). This is consistent with the fact that additional proteins containing a SH3 domain also bind to dynamin (47). Second, a fusion protein consisting of GST and the SH3 domain of SNX33 with interacted endogenous dynamin-2, as determined in a pulldown experiment using HEK293 cell lysates (Fig. 7B). Third, co-transfection of SNX33 together with wild-type dynamin-1, which does not affect APP endocytosis (Fig. 1B), largely rescued the SNX33 effect on APP shedding (Fig. 7C). Together, these experiments indicate that SNX33 inhibits APP endocytosis by inhibiting dynamin function.

Transgenic Expression of SNX33 in C. elegans Induces a Dynamin Loss-of-function Phenotype—A dynamin loss-of-function phenotype was also observed in vivo using C. elegans, which has only one ortholog of SNX33, SNX9, and SNX18 termed *lst-4* (Fig. 2) (48). Transgenic animals were generated,



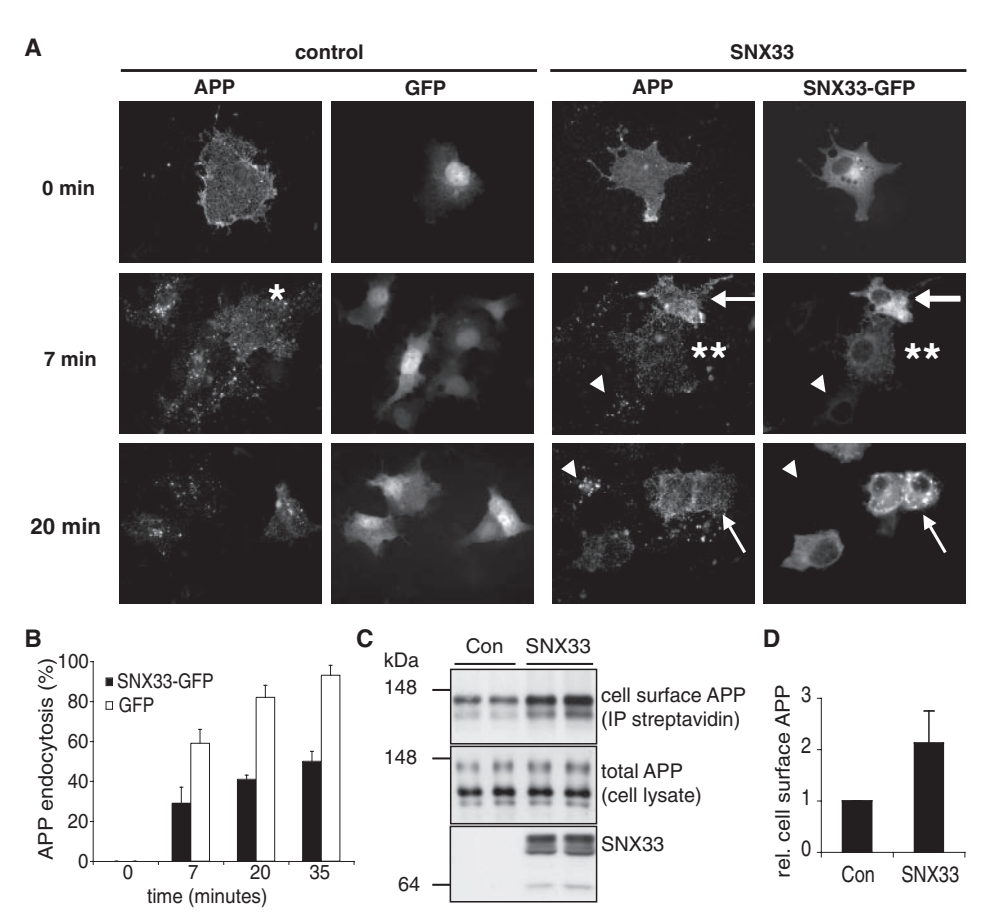
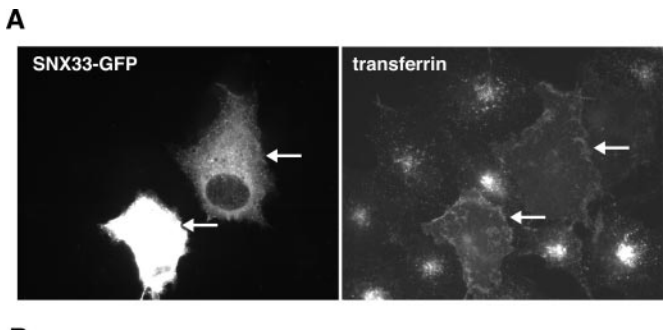


FIGURE 5. SNX33 inhibits APP endocytosis. A and B, COS cells were transiently co-transfected with APP and either SNX33-GFP or GFP as a control. Cells were incubated on ice (inhibition of endocytosis) with the polyclonal antibody 5313 against the extracellular domain of APP, washed, and returned to 37 °C (allowing endocytosis). After the indicated time points at 37 °C, cells were fixed, permeabilized, and stained with a fluorescently labeled secondary antibody against the primary anti-APP antibody. Cells were analyzed by fluorescence microscopy. A, first and third columns, fluorescence of APP. Second and fourth columns, fluorescence of GFP or SNX33-GFP. Top row, At time point 0 min, cells showed patchy cell surface staining of APP. Second and third rows (7 and 20 min), SNX33-GFP-expressing cells showed reduced levels of APP endocytosis in comparison with GFP-expressing cells. The GFP tag does not interfere with SNX33 function, as measured by its effect on APP α -cleavage (see Fig. 3B). The arrows point to cells that express SNX33 and show APP cell surface staining (no endocytosis). The arrowheads point to cells from the same transfection that express APP but no detectable SNX33; these cells showed endocytosis similar to the control cells. Note that at 7 min, the cells labeled with single and double asterisks have just started undergoing APP endocytosis (APP-positive vesicles and additionally remaining APP cell surface staining can be seen). Shown are representative pictures of three independent experiments. B, around 100 cells expressing GFP or SNX33-GFP were analyzed at every time point and scored as showing or not showing APP endocytosis. Given are the mean and the S.D. of three independent experiments. Cells were counted under blind conditions. C, cell surface biotinylation assay. HEK293 cells were transiently transfected with the indicated constructs. Endogenous cell surface APP was biotinylated, immunoprecipitated (IP), and detected by immunoblot using APP antibody 6687. Expression of SNX33 was detected using HA antibody. D, quantification of the blot from 5C. Mean and S.D. of three independent experiments are shown, each one carried out in duplicate.

which express GFP-tagged lst-4 cDNA (Ex[lst-4::gfp]) under the control of a 2.4-kb lst-4 upstream regulatory sequence. Remarkably, only few out of 200 injected animals survived and developed like wild-type worms, having normal brood size at 20 °C. This indicates that exogenous lst-4 expression interfered with viability and development of C. elegans, as is expected for a protein inhibiting endocytosis. Nevertheless, two stable transgenic lines (Ex[lst-4::gfp] lines 1 and 2) could be established, which again showed severely reduced brood size compared with wild-type animals (data not shown). Next, we compared the development of the two surviving transgenic lines with wild-type animals and with animals carrying a temperature-sensitive loss-of-function mutation in the single C. elegans

dynamin gene (dyn-1(ky51)) (49). Fertilized C. elegans eggs develop through four larval stages (L1, L2, L3, and L4) to adulthood. Eggs were laid at 15 °C and then moved to 26 °C, which is the restrictive temperature for the dynamin mutant animals. After 2 days of development, essentially all wild-type worms had developed normally and were found either in adulthood or in L4 larval stage (99.9%; Table 1 and Fig. 8A). In contrast, dynamin mutant animals showed a severe developmental phenotype at this restrictive temperature. Only a few animals (1.4%) developed normally, whereas most animals (76%) arrested at L1 or L2, and only 13.9% reached the L3 larval stage (Table 1), in agreement with a previous report (49). The L1/L2-arrested and L3 larval animals had thin and clear bodies compared with wild-type animals, sometimes accompanied by deformed body regions (Fig. 8B). Furthermore, \sim 9% of the progeny died during embryogenesis, which is in line with a previous publication (49). The two surviving transgenic *lst-4* lines showed a phenotype resembling the phenotype induced by mutation of the dynamin gene dyn-1. In detail, 15.4% of the surviving Ex[lst-4::gfp] worms (line 1) arrested at L1/L2 and 18.4% reached the L3 larval stage. This distribution was accompanied by phenotypic changes, which were very similar to the changes observed in the surviving dynamin mutant animals, such as deformed bodies appearing lumpy, especially in head and tail regions (Table 1 and Fig. 8C). Larvae with

extensively deformed bodies died after 72 h at 26 °C. Transgenic line 2 gave similar results as line 1 (Table 1 and Fig. 8*D*). Moreover, the transgenic *lst-4* and the *dyn-1(ky51)* mutant animals showed a similar reduction of life span (life span for Ex[lst-4::gfp] was 10.7 ± 0.2 days (n=100), and life span for dyn-1(ky51) was 9.9 ± 0.3 days (n=58)) compared with wild-type animals (13.6 ± 0.4 days (n=50)), which is a life span reduction of ~21 and ~27%, respectively. To further elucidate the functional interaction of the two proteins DYN-1 and LST-4, dyn-1-overexpressing animals (Ex[dyn-1a/b::gfp]; see Ref. 50) were crossed into Ex[lst-4::gfp] and phenotypically analyzed at 26 °C. Indeed, overexpression of dyn-1 could rescue the developmental defects of the Ex[lst-4::gfp] animals almost com-



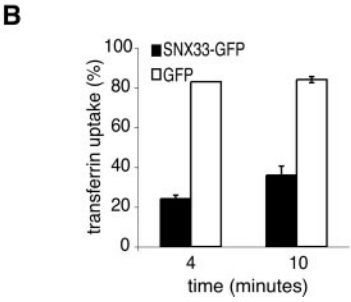


FIGURE 6. SNX33 inhibits uptake of transferrin. A and B, COS cells were transiently transfected with SNX33-GFP or GFP as a control. Cells were incubated with Alexa555-Fluor-coupled transferrin. Cells were returned for 4 or 10 min to 37 °C, fixed, and analyzed by fluorescence microscopy. Shown are SNX33-GFP-transfected cells at the 10 min time point. Left, GFP fluorescence; right, transferrin. The arrows mark cells that express SNX33-GFP and do not show endocytosis at this time point. Nontransfected cells (expressing endogenous transferrin receptor) show transferrin uptake (endocytic vesicles). Around 100 cells expressing SNX33-GFP (black bars) or GFP (white bars) were analyzed for every time point and scored as showing transferrin uptake or not. The graph shows the mean of three independent experiments.

pletely (Table 1). Taken together, the low number of surviving transgenic *lst-4* animals as well as the analyses of development and life span show that the Ex[lst-4::gfp] phenotype is similar to the phenotype of *dyn-1(ky51)* mutant animals. Moreover, our results show that the phenotype can be rescued by overexpression of wild-type *dyn-1a/b::gfp*. This indicates that overexpression of lst-4 results in a phenotype very similar to a dynamin loss-of-function phenotype in *C. elegans*, demonstrating the functional interaction between these two proteins.

DISCUSSION

Changes in endocytic trafficking can modulate APP shedding by α - and β -secretase and are associated with early neuropathological changes observed in AD brain (15). However, the detailed mechanisms controlling APP endocytosis and the availability of APP to both secretases are only partly understood. Here, we identified the novel SNX33 as a new protein involved in endocytosis and showed that it modulates APP endocytosis and shedding. SNX33 inhibited dynamin function, resulting in decreased APP endocytosis and increased APP cell surface levels, where it underwent enhanced cleavage by α -secretase, which mainly cleaves at the plasma membrane (46).

The cellular regulation of APP α -secretase cleavage is of great interest, because α -secretase cleaves within the A β domain and reduces the amount of APP available for β -secretase cleavage and A β generation. Additionally, α -secretase cleavage generates a large soluble APP ectodomain (APPs α), which has neuroprotective and neurotrophic properties (6-8). Moreover, APPs α seems to mediate the physiological functions

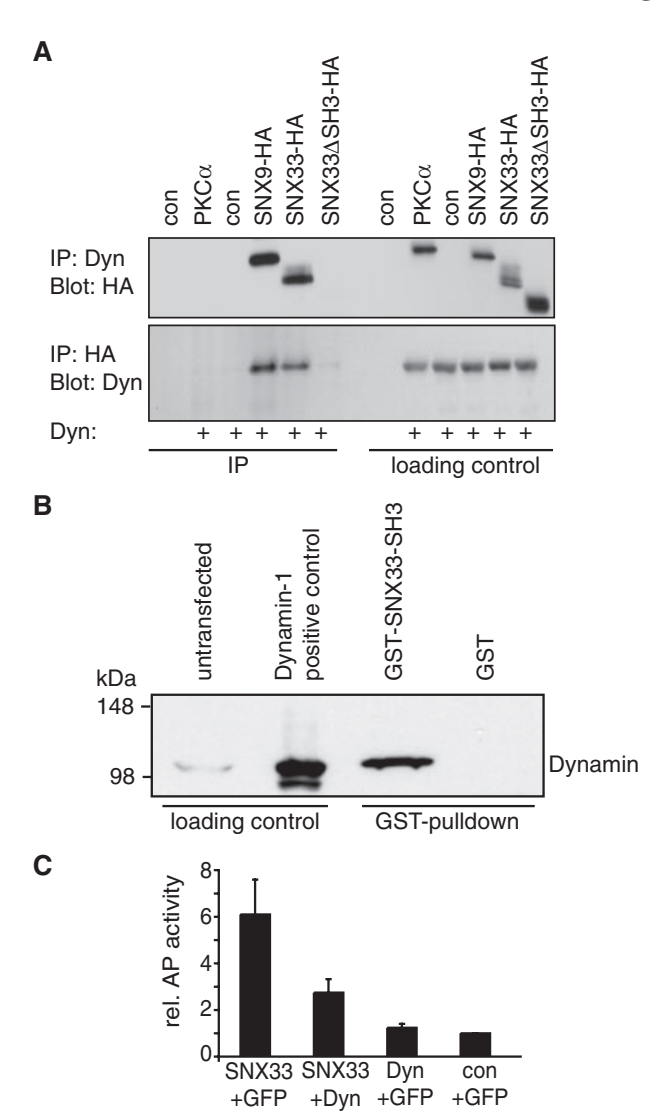


FIGURE 7. SNX33 co-immunoprecipitates with dynamin. A, HEK293 cells were transiently co-transfected with dynamin-1 and the indicated constructs. SNX33 as well as SNX9 co-immunoprecipitate with dynamin-1, whereas the deletion mutant SNX33-ΔSH3 does not. An empty control vector (con) and the transfection of protein kinase $C\alpha$ were used as a control for specificity. Immunoprecipitated proteins were analyzed by immunoblot using the indicated antibodies. IP, immunoprecipitation with the indicated antibody; loading control, aliquots of the cell lysates were directly loaded. B, a fusion protein of GST and the SNX33 SH3 domain but not GST alone pulls down endogenous dynamin-2 from HEK293 cell lysates. As a control, cell extracts from untransfected (weak band of endogenous dynamin-2) or dynamin-1-transfected HEK293 cells were loaded. C, co-expression of wild-type dynamin-1 (Dyn) reduces the shedding-enhancing effect of SNX33. Human embryonic kidney cells stably expressing alkaline phosphatase-tagged APP were transiently cotransfected with the indicated constructs. AP activity in the conditioned medium was measured relative to control-transfected cells (with empty control vector (con) and GFP). Shown are the mean and S.D. of three independent experiments.

of the APP protein, because APPs α largely rescues the deficits observed in APP knock-out mice (51).

 α -Secretase cleavage of APP and secretion of APPs α can be strongly enhanced by different stimuli (9), but the underlying molecular and cellular mechanisms are largely unknown. For the proteins identified in this screen and in a previous one (31), we found that the strongest increase in α -secretase cleavage was observed for proteins, which reduced the rate of APP endocytosis. This suggests that the rate of APP endocytosis is a cen-



TABLE 1 Comparison of Ce Ist-4 transgenic and dynamin mutant animals

Strain	Phenotype of progeny at 26 °C				
	L4 larvae and adult	L3 larvae	L1/L2 arrest	Dead eggs	No.a
	%	%	%	%	
Wild type	99.9	0	0	0.1	1013
Ex[lst-4::gfp] line1	63.2	18.4	15.4	3.0	749
Ex[lst-4::gfp] line2	71.0	6.6	11.0	11.4	977
dyn-1(ky51)	1.4	13.9	76.0	8.7	840
$Ex[dyn-1a/b::gfp]^b$	98.6	0.4	0.7	0.3^{c}	790
$\operatorname{Ex}[dyn-1a/b::gfp; lst-4::gfp]^d$	94.6	1.1	1.0	3.3^{c}	807

^a Total number of animals scored after 48 h.

^d To generate BR4825, Ex[lst-4::gfp] line1 was crossed into ZH301.

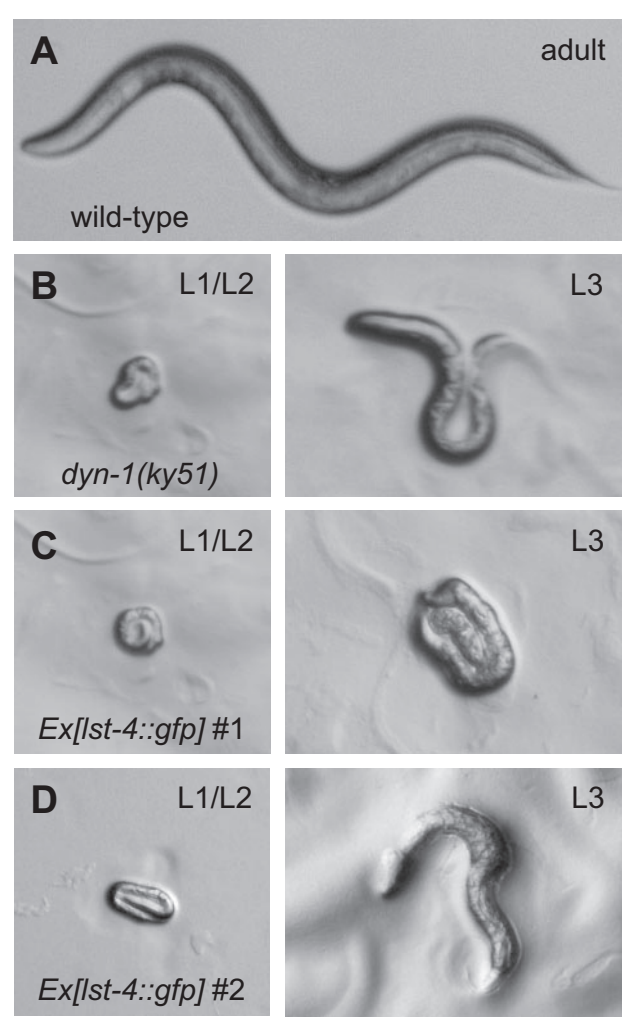


FIGURE 8. Phenotypic analysis of dynamin mutant and Ist-4 transgenic C. elegans. Shown are representative images of the following four different C. elegans strains. A, wild-type adult animal. B, L1/L2 larva (left) and L3 larva (right) of dyn-1(ky51) mutant. C, L1/L2 larva (left) and L3 larva (right) of transgenic Ex[lst-4::qfp] line 1. D, L1/L2 larva (left) and L3 larva (right) of transgenic $E_X[Ist-4::gfp]$ line 2. For phenotypic analysis (see also Table 1), worms were allowed to lay eggs for 2 h at 15 °C before being removed. Eggs were shifted to 26 °C, incubated for 48 h, and analyzed using a Zeiss Imager.Z1. Images were collected with an Olympus Camedia C-5060 microscope. The same magnifications were used for all images.

tral factor determining how much APP is available for α -secretase cleavage. SNX33 and Dyn Δ NT (this study), endophilin A3 (31), and the APP homolog APLP1 (32) increased APP α -secretase cleavage more than 4-fold, whereas expression of the α -secretase ADAM10 or of different kinases, such as protein kinase A or a constitutively active form of MEKK2 increased APP shedding 2-fold at most (31). The only other protein identified that strongly increased APP shedding was the β -secretase BACE1 (this study), which increases APP shedding 6-fold (31), but this was due to an increase in β -secretase and not in α -secretase cleavage. The identified proteins reduced APP endocytosis through different molecular mechanisms but increased APP α -secretase cleavage to a similar extent. SNX33, endophilin A3, and DynΔNT reduced general dynamin-dependent endocytosis, including that of APP. In contrast, APLP1 selectively inhibited APP endocytosis by reducing complex formation between APP, FE65, and LRP (32). Formation of this complex is required for the normal rate of APP endocytosis. Two previous studies used the well characterized dominant-negative dynamin-1 K44A mutant and also reported an increase in APP α -secretase cleavage (12, 13). The only study that did not report an increase in APP α -secretase cleavage upon dynamin K44A expression did not use wild-type APP but rather the Swedish mutant APP (45), which is known to be mainly cleaved in the secretory pathway and seems to depend to a different extent on endocytosis for its β -secretase cleavage compared with wild-type APP (52). Together, these data show that the rate of APP endocytosis is a major control factor for the amount of APP α -secretase cleavage. Moreover, our results show that not only dynamin but also other endocytic proteins, such as SNX33, can contribute to the modulation of APP endocytosis and α -secretase cleavage.

For β -secretase cleavage, the consequences of a reduction of APP endocytosis are less clear than for α -secretase, and conflicting results have been reported previously (12, 13). α - and β -secretase are assumed to compete for the shedding of APP, suggesting that an increased shedding by α -secretase is accompanied by a reduction in β -secretase cleavage, and *vice versa*. Surprisingly, we found that this is not always the case. Looking at endogenous APP in HEK293 cells we found that both SNX33 and Dyn K44A increased α -secretase but did not affect or even modestly increase β -secretase cleavage. Similar results for SNX33 were obtained in HeLa and H4 cells. Likewise, one of the previous studies, which analyzed shedding of endogenous APP in HeLa cells, found that Dyn K44A increased APP α -cleavage. APP β -cleavage was also enhanced, although to a lower extent than α -cleavage (13). Together, these findings reveal that a general inhibition of endocytosis strongly increases APP α -secretase cleavage and mildly increases APP β -secretase cleavage, at least for endogenous APP.

b ZH301 unc-76(e911); enEx38; see Ref. 50.

^c The genotype of the dead eggs is different depending on the presence/absence of the extrachromosomal arrays.

Endocytosis requires the orchestration of different regulatory proteins in a time- and space-dependent manner and is a highly regulated process (16-18). Although several regulators of endocytic trafficking, such as dynamin and Rab5, are known, not all molecular mechanisms and proteins controlling endocytosis have been identified. Our study reveals that SNX33 is a novel protein involved in endocytic trafficking, thus expanding the number of proteins contributing to this process. SNX33 is a new binding partner of dynamin, which is a key component of endocytosis (16). Dynamin is also involved in synaptic vesicle recycling, and loss-of-function mutations in the ubiquitously expressed dynamin-2 causes specific forms of the Charcot-Marie-Tooth disease type 2 neuropathy (53, 54). SNX33 expression induced a dynamin loss-of-function phenotype in cultured cells, where we observed an inhibition of APP endocytosis and also of transferrin uptake, suggesting a broader role for SNX33 in dynamin-dependent endocytosis. This is further supported by the in vivo experiments in C. elegans, where the SNX33 ortholog *lst-4* induced a dynamin loss-of-function phenotype. The interaction between SNX33 and dynamin requires the SH3 domain of SNX33, which most likely binds to the proline-rich domain of dynamin. Other SH3 domain-containing proteins also bind to this domain in dynamin, and these proteins are involved in different steps of endocytosis (47). Thus, it seems likely that an increase in SNX33 expression, for example by transgenic expression, partly prevents dynamin from the other protein interactions required for efficient endocytosis, resulting in a dynamin loss-of-function phenotype. Interestingly, a similar situation may occur in vivo. In C. elegans, expression of the SNX33 ortholog lst-4 can be strongly increased during development of vulva precursor cells (48). If a similar regulation of expression holds true for human SNX33 or its homologs, this would be expected to alter APP endocytosis and shedding.

SNX9 has the same domain structure as SNX33 but has only 50% similarity in the amino acid sequence. Nevertheless, we found SNX9 to have a similar effect on APP shedding and APP cell surface levels as SNX33. Moreover, SNX9 is also involved in endocytic trafficking. SNX9 binds dynamin (22, 23) and other proteins involved in endocytosis, such as synaptojanin and the actin-remodeling proteins WASP and N-WASP (40-42). SNX9 is involved in transferrin uptake (23) and in membrane localization of dynamin (39) and modulates N-WASP-dependent actin assembly in different forms of endocytosis (42). Additionally, SNX9 transfection blocks synaptic vesicle endocytosis in neurons (55). SNX33 and SNX9 have a third distant homolog, called SNX18, which has not yet been characterized. Potentially, these three SNXs constitute a subgroup of the SNX family with a function in endocytosis.

In summary, our study identifies SNX33 as a new endocytic protein, which modulates APP endocytosis and APP α -secretase cleavage, and demonstrates that APP endocytosis is a major control factor for APP α -secretase cleavage.

Acknowledgments—We thank Suzanne Pfeffer for helpful comments on the manuscript and Katrin Moschke and Anne Oelmann for excellent technical help.

REFERENCES

- 1. Selkoe, D. J., and Schenk, D. (2003) Annu. Rev. Pharmacol. Toxicol. 43, 545-584
- 2. Citron, M. (2004) Trends Pharmacol. Sci. 25, 92-97
- 3. Haass, C. (2004) EMBO J. 23, 483-488
- 4. Allinson, T. M., Parkin, E. T., Turner, A. J., and Hooper, N. M. (2003) J. Neurosci. Res. 74, 342-352
- 5. Skovronsky, D. M., Moore, D. B., Milla, M. E., Doms, R. W., and Lee, V. M. (2000) J. Biol. Chem. 275, 2568-2575
- 6. Furukawa, K., Sopher, B. L., Rydel, R. E., Begley, J. G., Pham, D. G., Martin, G. M., Fox, M., and Mattson, M. P. (1996) J. Neurochem. 67, 1882–1896
- 7. Meziane, H., Dodart, J. C., Mathis, C., Little, S., Clemens, J., Paul, S. M., and Ungerer, A. (1998) Proc. Natl. Acad. Sci. U. S. A. 95, 12683–12688
- 8. Stein, T. D., Anders, N. J., DeCarli, C., Chan, S. L., Mattson, M. P., and Johnson, J. A. (2004) J. Neurosci. 24, 7707-7717
- 9. Huovila, A. P., Turner, A. J., Pelto-Huikko, M., Karkkainen, I., and Ortiz, R. M. (2005) Trends Biochem. Sci. 30, 413-422
- 10. Koo, E. H., and Squazzo, S. L. (1994) J. Biol. Chem. 269, 17386 -17389
- 11. Haass, C., Hung, A. Y., Schlossmacher, M. G., Oltersdorf, T., Teplow, D. B., and Selkoe, D. J. (1993) J. Biol. Chem. 268, 3021-3024
- 12. Carey, R. M., Balcz, B. A., Lopez-Coviella, I., and Slack, B. E. (2005) BMC Cell Biol. 6, 30
- 13. Chyung, J. H., and Selkoe, D. J. (2003) J. Biol. Chem. 278, 51035-51043
- 14. Grbovic, O. M., Mathews, P. M., Jiang, Y., Schmidt, S. D., Dinakar, R., Summers-Terio, N. B., Ceresa, B. P., Nixon, R. A., and Cataldo, A. M. (2003) J. Biol. Chem. 278, 31261-31268
- 15. Nixon, R. A. (2005) Neurobiol. Aging 26, 373–382
- 16. Le Roy, C., and Wrana, J. L. (2005) Nat. Rev. 6, 112-126
- 17. Mayor, S., and Pagano, R. E. (2007) Nat. Rev. 8, 603-612
- 18. Zerial, M., and McBride, H. (2001) Nat. Rev. 2, 107-117
- 19. Worby, C. A., and Dixon, J. E. (2002) Nat. Rev. 3, 919-931
- 20. Carlton, J., Bujny, M., Rutherford, A., and Cullen, P. (2005) Traffic 6,
- 21. Teasdale, R. D., Loci, D., Houghton, F., Karlsson, L., and Gleeson, P. A. (2001) Biochem. J. 358, 7–16
- 22. Lundmark, R., and Carlsson, S. R. (2003) J. Biol. Chem. 278, 46772-46781
- Soulet, F., Yarar, D., Leonard, M., and Schmid, S. L. (2005) Mol. Biol. Cell **16,** 2058 – 2067
- 24. Steiner, H., Kostka, M., Romig, H., Basset, G., Pesold, B., Hardy, J., Capell, A., Meyn, L., Grim, M. L., Baumeister, R., Fechteler, K., and Haass, C. (2000) Nat. Cell Biol. 2, 848 – 851
- 25. Ida, N., Hartmann, T., Pantel, J., Schröder, J., Zerfass, R., Förstl, H., Sandbrink, R., Masters, C. L., and Beyreuther, K. (1996) J. Biol. Chem. 271, 22908 - 22914
- 26. Lammich, S., Schobel, S., Zimmer, A. K., Lichtenthaler, S. F., and Haass, C. (2004) EMBO Rep. 5, 620-625
- 27. Lichtenthaler, S. F., Ida, N., Multhaup, G., Masters, C. L., and Beyreuther, K. (1997) Biochemistry 36, 15396-15403
- 28. Lichtenthaler, S. F., Dominguez, D. I., Westmeyer, G. G., Reiss, K., Haass, C., Saftig, P., De Strooper, B., and Seed, B. (2003) J. Biol. Chem. 278, 48713-48719
- 29. Lichtenthaler, S. F. (2006) Neurodegener. Dis. 3, 262-269
- 30. Kuhn, P. H., Marjaux, E., Imhof, A., De Strooper, B., Haass, C., and Lichtenthaler, S. F. (2007) J. Biol. Chem. 282, 11982–11995
- 31. Schobel, S., Neumann, S., Seed, B., and Lichtenthaler, S. F. (2006) Int. J. Dev. Neurosci. 24, 141-148
- 32. Neumann, S., Schobel, S., Jager, S., Trautwein, A., Haass, C., Pietrzik, C. U., and Lichtenthaler, S. F. (2006) J. Biol. Chem. 281, 7583-7594
- 33. Mello, C. C., Kramer, J. M., Stinchcomb, D., and Ambros, V. (1991) EMBO *J.* **10,** 3959 – 3970
- 34. Vassar, R., Bennett, B. D., Babu-Khan, S., Kahn, S., Mendiaz, E. A., Denis, P., Teplow, D. B., Ross, S., Amarante, P., Loeloff, R., Luo, Y., Fisher, S., Fuller, J., Edenson, S., Lile, J., Jarosinski, M. A., Biere, A. L., Curran, E., Burgess, T., Louis, J. C., Collins, F., Treanor, J., Rogers, G., and Citron, M. (1999) Science 286, 735-741
- 35. Herskovits, J. S., Burgess, C. C., Obar, R. A., and Vallee, R. B. (1993) J. Cell Biol. 122, 565-578



- 36. Seet, L. F., and Hong, W. (2006) Biochim. Biophys. Acta 1761, 878 896
- 37. Smalley, D. M., and Ley, K. (2005) J. Cell Mol. Med. 9, 255-266
- 38. Peschon, J. J., Slack, J. L., Reddy, P., Stocking, K. L., Sunnarborg, S., Lee, D. C., Russell, W. E., Castner, B. J., Johnson, R. S., Fitzner, J. N., Boyce, R. W., Nelson, N., Kozlosky, C. J., Wolfson, M. F., Rauch, C. T., Cerretti, D. P., Paxton, R. J., March, C. J., and Black, R. A. (1998) Science **282,** 1281-1284
- 39. Lundmark, R., and Carlsson, S. R. (2004) J. Biol. Chem. 279, 42694 42702
- 40. Badour, K., McGavin, M. K., Zhang, J., Freeman, S., Vieira, C., Filipp, D., Julius, M., Mills, G. B., and Siminovitch, K. A. (2007) Proc. Natl. Acad. Sci. U. S. A. 104, 1593-1598
- 41. Worby, C. A., Simonson-Leff, N., Clemens, J. C., Kruger, R. P., Muda, M., and Dixon, J. E. (2001) J. Biol. Chem. 276, 41782-41789
- 42. Yarar, D., Waterman-Storer, C. M., and Schmid, S. L. (2007) Dev. Cell 13,
- 43. Dawson, J. C., Legg, J. A., and Machesky, L. M. (2006) Trends Cell Biol. 16, 493 - 498
- 44. Childress, C., Lin, Q., and Yang, W. (2006) Biochem. J. 394, 693-698
- 45. Ehehalt, R., Keller, P., Haass, C., Thiele, C., and Simons, K. (2003) J. Cell Biol. 160, 113–123

- 46. Sisodia, S. S. (1992) Proc. Natl. Acad. Sci. U. S. A. 89, 6075–6079
- 47. Hinshaw, J. E. (2000) Annu. Rev. Cell Dev. Biol. 16, 483-519
- 48. Yoo, A. S., Bais, C., and Greenwald, I. (2004) Science 303, 663-666
- 49. Clark, S. G., Shurland, D. L., Meyerowitz, E. M., Bargmann, C. I., and van der Bliek, A. M. (1997) Proc. Natl. Acad. Sci. U. S. A. 94, 10438-10443
- 50. Yu, X., Odera, S., Chuang, C. H., Lu, N., and Zhou, Z. (2006) Dev. Cell 10, 743-757
- 51. Ring, S., Weyer, S. W., Kilian, S. B., Waldron, E., Pietrzik, C. U., Filippov, M. A., Herms, J., Buchholz, C., Eckman, C. B., Korte, M., Wolfer, D. P., and Muller, U. C. (2007) J. Neurosci. 27, 7817-7826
- 52. Haass, C., Lemere, C. A., Capell, A., Citron, M., Seubert, P., Schenk, D., Lannfelt, L., and Selkoe, D. J. (1995) Nat. Med. 1, 1291-1296
- 53. Fabrizi, G. M., Ferrarini, M., Cavallaro, T., Cabrini, I., Cerini, R., Bertolasi, L., and Rizzuto, N. (2007) Neurology 69, 291-295
- 54. Zuchner, S., Noureddine, M., Kennerson, M., Verhoeven, K., Claeys, K., De Jonghe, P., Merory, J., Oliveira, S. A., Speer, M. C., Stenger, J. E., Walizada, G., Zhu, D., Pericak-Vance, M. A., Nicholson, G., Timmerman, V., and Vance, J. M. (2005) Nat. Genet. 37, 289-294
- Shin, N., Lee, S., Ahn, N., Kim, S. A., Ahn, S. G., Park, Z. Y., and Chang, S. (2007) J. Biol. Chem. 282, 28939-28950

A Novel Sorting Nexin Modulates Endocytic Trafficking and α -Secretase Cleavage of the Amyloid Precursor Protein

Susanne Schöbel, Stephanie Neumann, Maren Hertweck, Bastian Dislich, Peer-Hendrik Kuhn, Elisabeth Kremmer, Brian Seed, Ralf Baumeister, Christian Haass and Stefan F. Lichtenthaler

J. Biol. Chem. 2008, 283:14257-14268. doi: 10.1074/jbc.M801531200 originally published online March 19, 2008

Access the most updated version of this article at doi: 10.1074/jbc.M801531200

Alerts:

- When this article is cited
- When a correction for this article is posted

Click here to choose from all of JBC's e-mail alerts

This article cites 55 references, 27 of which can be accessed free at http://www.jbc.org/content/283/21/14257.full.html#ref-list-1